Utilizing the Discrete Orthogonality of Zernike Functions in Corneal Measurements

Zoltán Fazekas, Alexandros Soumelidis * and Ferenc Schipp †

Abstract—**The optical behaviour of the human eye is often characterized with the Zernike coefficients. Great number of measurements and statistical data are available for individuals and for various groups of people concerning the Zernike coefficients of their eyes. Although, these coefficients were obtained from measurements at discrete points and via computations using some discretization of the continuous Zernike functions, the developers of these algorithms could not rely on the discrete orthogonality Zernike functions, simply because no mesh of points ensuring discrete orthogonality was known. Only recently was such a mesh of points found and reported. In the present paper, this mesh is used to calculate Zernike coefficients for some artificial cornea-like surfaces. Tests were carried out and are reported herein on the precision of the discrete orthogonality obtained via the mentioned discretization and on the precision of the surface reconstruction.**

Keywords: corneal topography, discrete orthogonal systems, Zernike functions

1 Introduction

The orthogonal system of Zernike functions were introduced in [1] to model symmetries and aberrations of optical systems (e.g., telescopes). In Fig. 1, one of the Zernike functions is shown as an example in pseudo-colour. Some of the important and useful properties of the Zernike-system are summarized in [8]. The mentioned paper can be used as a pointer to a wider range of relevant publications. In Section 2, the continuous Zernike functions and their indexing used in this paper are presented.

1.1 Zernike Functions in Ophthalmology

Nowadays, the ophthalmologists are quite familiar with the smoothly curving Zernike-surfaces. They use these surfaces exactly in the way as was intended by Zernike, that is, to describe various symmetries and aberrations of an optical system. In their case, of the human eye, more precisely, of the corneal surface – measured with some corneal topographer – and of the refractive properties of the eyeball (measured e.g., with a Shack-Hartmann wavefront-sensor). This description is given in the form of Zernike coefficients.

As the optical aberrations may cause serious acuity problems, and are significant factors to be considered in planning of sight-correcting operations, wide range of statistical data – concerning the eyes of various groups of people – is available for the most important Zernike coefficients [11].

Another interesting use of the Zernike coefficients was reported recently. The optical aberrations of the eye make it difficult or in certain cases impossible to make high-resolution retinal images without compensating these aberrations. However, by compensating them the high-resolution retinal imaging can be achieved [12].

1.2 Placido Disks and Other Measurement Patterns

The purpose of a cornea topographic examination is to determine and display the shape and the optical power of the living cornea. Due to the high refractive power of the human cornea, the knowledge of its detailed topography is of great diagnostic importance. The corneal surface is often modelled as a spherical calotte, though, more complex surface models are also used for various purposes, including testing corneal topographer with non-spherical surfaces [10]. Such test surfaces are shown in Figs. 5, 6 and 7.

The monocular cornea topographers evaluate the virtual image of some measurement pattern that is reflected and – after reflection – somewhat distorted by the corneal surface. Many of the reflection-based corneal topographers use a system of bright and dark concentric rings, called Placido disk, as measurement-pattern. Such a measurement pattern and its more sophisticated colour variant are shown in Fig. 2.

The measurement properties of the conventional Placido disk based topographers are rather problematic, as no point-to-point correspondences are available for the purpose of surface reconstruction [4]. On the other hand, the reflection-based monocular corneal topographers with

*Z. Fazekas and A. Soumelidis are with the Computer and Automation Research Institute, Hungarian Academy of Sciences, Budapest, Hungary, Email: {zfazekas, soumelidis}@sztaki.hu

†F. Schipp is with the Eötvös Loránd University, Department of Numerical Analysis, Budapest, Hungary, Email: schipp@ludens.elte.hu

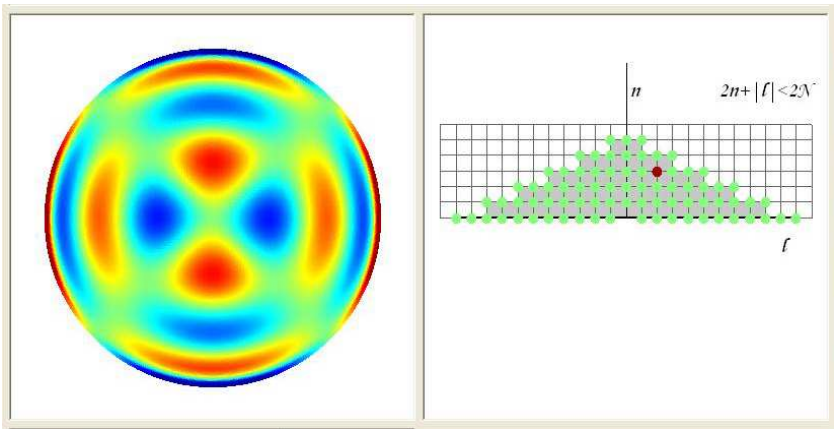

Figure 1: An example of the Zernike functions, namely Y_3^2. Its indices can be verified in the index-space shown on the right.

more elaborate and more distinguishable measurement patterns are still popular, though they often rely on manual positioning and on some means to mark a surface-point.

Recently, a multi-camera surface reconstruction method was suggested for the purpose of corneal topography in [14]. The reconstruction is achieved by solving the partial differential equations describing the specular reflections at the corneal surface. Though the multi-camera corneal measurement approach is more precise and more robust than the monocular measurements, the monocular corneal topographers are nevertheless expected to remain in use. For this reason, it is worth noting that the discrete mesh of Fig. 3 – proposed in [8] – could well be considered for the purpose of monocular corneal measurements.

1.3 Utilizing Discrete Orthogonality

Although, Zernike coefficients were obtained from measurements at discrete corneal points and via computations using some discretization of the continuous Zernike functions, the developers of these algorithms could not rely on the discrete orthogonality – see e.g., [5], [6] – Zernike functions simply because no mesh of points ensuring discrete orthogonality was known. Not surprisingly, the discrete orthogonality of Zernike functions was a target of research for some decades [3] and only recently was a mesh of points – ensuring discrete orthogonality of the Zernike functions – found and introduced [8].

In the present paper, the aforementioned mesh is used to calculate the Zernike coefficients for some artificial cornea-like surfaces. Tests were carried out on the precision of the discrete orthogonality obtained via the mentioned discretization and on the precision of reconstruction from the Zernike coefficients.

In Section 3, the discretization approach introduced in [8] is presented briefly. In Section 4, the program implementation of the discrete Zernike functions is presented – together with programs for testing the orthogonality of these functions, for computing the Zernike coefficients of a surface. Finally, we draw conclusions in Section 5.

2 Continuous Zernike Functions

A surface over the unit disk can be described by a two-variable function $g(x, y)$. The application of the polar-transform to variables x and y results in

$$x = \rho\cos\vartheta, \quad y = \rho\sin\vartheta, \tag{1}$$

where ρ and ϑ are the radial and the azimuthal variables, respectively, over the unit disk, i.e., where

$$0 \le \rho \le 1, \quad 0 \le \vartheta \le 2\pi. \tag{2}$$

Using ρ and ϑ, $g(x, y)$ can be transcribed in the following form:

$$G(\rho, \vartheta) := g(\rho\cos\vartheta, \rho\sin\vartheta). \tag{3}$$

The set of Zernike polynomials of degree less than 2N is as follows.

$$Y_n^l(\rho, \vartheta) := \sqrt{2n + |l| + 1} \cdot R^{|l|}_{|l|+2n}(\rho) \cdot e^{il\vartheta}$$
$$(l \in \mathbb{Z}, n \in \mathbb{N}, |l| + 2n < 2N) \tag{4}$$

The radial polynomials $R^{|l|}_{|l|+2n}$ can be expressed with the Jacobi polynomials $P_k^{\alpha,\beta}$ in the following manner:

$$R^{|l|}_{|l|+2n}(\rho) = \rho^{|l|} \cdot P_n^{0,|l|}(2\rho^2 - 1). \tag{5}$$

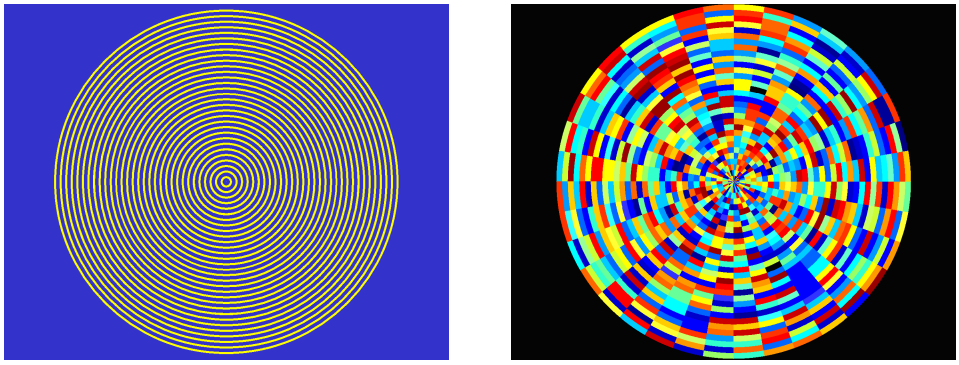

Figure 2: The Placido disk and its more sophisticated random-coloured version.

For example, $R_0^0 = 1$, $R_2^0 = 2\rho^2 - 1$, $R_4^0 = 6\rho^4 - 6\rho^2 + 1$ and $R_1^1 = \rho$, $R_3^1 = 3\rho^3 - 2\rho$.

In Fig. 1, a particular Zernike function – namely Y_3^2 – is shown in a pseudo-colour representation. In the right-hand-side of the figure, the index-space is shown for $N = 6$, that is, for the set of Zernike polynomials of degree less than 12. The point $(2, 3)$ – corresponding to the indices of the particular Zernike function Y_3^2 – is shown as a red dot in the index-space.

3 Discretization of Zernike Functions

3.1 The Mesh Ensuring the Discrete Orthogonality of Zernike Functions

The mesh, i.e., the set of nodal points – given in [8] and proven to ensure the discrete orthogonality of Zernike functions over this mesh – is as follows:

$$X_N := \{z_{jk} := (\rho_k^N, \frac{2\pi j}{4N+1}) : k = 1, ..., N, j = 0, .., 4N\}, \tag{6}$$

where

$$\rho_k^N := \sqrt{\frac{1+\lambda_k^N}{2}}, \quad k = 1, ..., N. \tag{7}$$

In (7), λ_k^N is the k-th root ($k = 1, ..., N$) of the Legendre polynomial P_N of order N. In Fig. 3, X_8 is shown as an example.

By using the discrete integral of (8), the discrete orthogonality of the Zernike functions can be proven. The discrete orthogonality relation is given in (9).

$$\int_{X_N} f(\rho, \phi) d\nu_N := \sum_{k=1}^{N} \sum_{j=0}^{4N} f(\rho_k^N, \frac{2\pi j}{4N+1}) \frac{A_k^N}{2(4N+1)} \tag{8}$$

In (8), the A_k^N's are the weights that are associated with the discrete circular rings in the mesh (e.g., with the discrete rings in the particular mesh shown in Fig. 3). In the right side of the figure, the weights A_k^8's are shown. These weights are derived for the radial Zernike polynomials from the quadrature formula of Legendre polynomials P_N of order N by argument transform. We note here that another argument transform – used in conjunction with another corneal surface description approach – was proposed in [9].

The quadrature formulas are significant tools in constructing discrete orthogonal systems. This is touched upon in Subsection 3.2.

$$\int_X Y_n^m(\rho, \phi) \overline{Y_{n'}^{m'}(\rho, \phi)} d\nu_N = \delta_{nn'} \delta_{mm'}. \tag{9}$$

In the above orthogonality relation $n + n' + |m| < 2N$ and $n + n' + |m'| < 2N$ is assumed.

3.2 The Significance of the Quadrature Formulas in Discretization

Quadrature formulas are known for some well-researched continuous orthogonal polynomials – of certain importance – of one variable since Gauss's time. See e.g., [2] The quadrature formulas are expressed in the following way:

$$\int_{-1}^{1} f(x) dx \approx \sum_{k=1}^{N} f(\lambda_k^N) A_k^N. \tag{10}$$

Interestingly, the integration of function $f(x)$ is much more precise than a numerical integration using over some arbitrary (e.g., equidistant mesh). In our case, that is, for the discretization of the radial Zernike polynomials – i.e., the radial component of the Zernike functions – the N roots of Legendre polynomials P_N were used. The exact formula for deriving the A_k^N weights is not given here, but we emphasize that the formula is exact for every

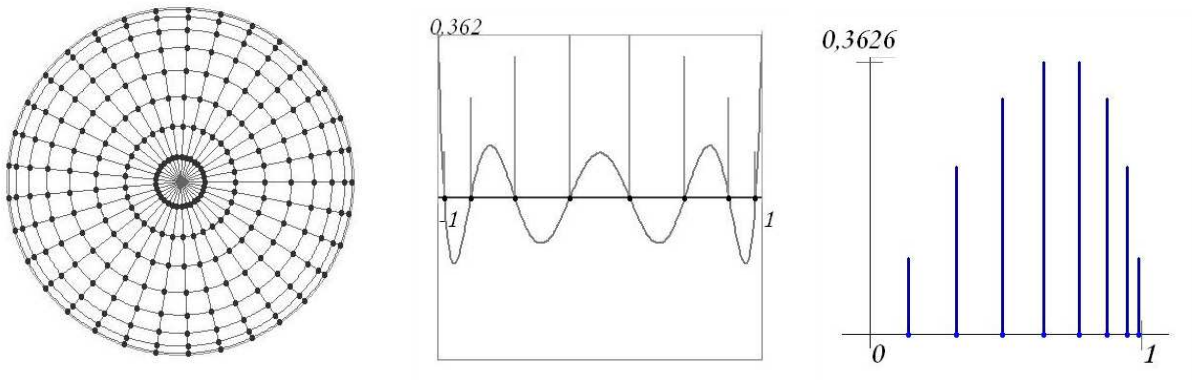

Figure 3: An example of the X_N mesh of points, namely X_8, that ensures the discrete orthogonality of Zernike functions over the mesh (left). As can be verified, this particular mesh contains $N(4N+1) = 8 * 33$ points. The weights – i.e., the Cristoffel numbers – appearing in the quadrature formula for Legendre polynomial P_8 (middle). The weights used in the discrete integral of (8) over mesh X_8 (right). Note that these weights are the same as the corresponding weights in the middle image, but the function is morphed by the argument transformation used in (5).

polynomial f of order less than $2N$, if the proper weights are used in the above summation.

In Fig. 3b, a particular Legendre polynomial, namely P_8 is shown. Its 8 roots fall in the interval $[-1, 1]$ and the weights $A_1^8, ..., A_8^8$ that should be used in the quadrature formula in (10) are indicated at the corresponding roots.

3.3 Precision Achieved

In order to check the mathematical calculations outlined above, a program implementation of the discrete Zernike functions was developed using standard double-precision floating point arithmetics. In Fig. 4, the user interface of this program is shown. With the marked indices input to the program, the aforementioned discrete orthogonality relation was checked for Zernike functions Y_5^3 and Y_1^9 and the discrete integral (9) was found to be about $3.8 \cdot 10^{-18}$.

4 The Discrete Zernike Coefficients

4.1 Computing the Discrete Zernike Coefficients

The discrete Zernike coefficients associated with function $T(\rho, \phi)$ can be calculated with the following discrete integral:

$$C_n^m = \frac{1}{\pi} \int_{X_N} T(\rho, \phi) \overline{Y_n^m(\rho, \phi)} d\nu_N. \qquad (11)$$

It is worth noting that if $T(\rho, \phi)$ happens to be an arbitrary linear combination of Zernike functions of degree less than $2N$, then the above discrete integrals, i.e., for n's and m's satisfying the inequality $2n + |m| < 2N$, result in the exact Zernike coefficients which are calculated from the corresponding continuous integrals.

4.2 Program Implementation for Computing Discrete Zernike Coefficients

The developed program implementation for computing the discrete Zernike coefficients was used to create Figs. 5, 6 and 7. The input functions were selected from the test-surfaces suggested by [10]. The reasons for selecting these three surfaces for illustrating the changes in the Zernike coefficients are as follows. Both Fig. 5 and Fig. 6 are sphero-cylindrical surfaces. This is clearly indicated by the two relatively strong low-order Zernike coefficients marked in each of the two figures. Note that the most significant Zernike coefficient C_0^0 is not shown in the figure to avoid the suppression of the other coefficients during normalization. By comparing the value – represented by the colour – of the two dots with the coordinates (0,1), one can see the change of strength in respect this coefficient between the two surfaces. Fig. 6 – on the other hand – was included here to show a surface with many active Zernike coefficients.

5 Conclusions and Future Work

The discretization used in this paper was proposed in [8]. It has relevance to the concrete application field, i.e., corneal measurements, but could also benefit physicists and engineers dealing with optical measurements, or with the design of optical measurement devices.

However, using this mesh directly, that is, using it as a measurement-pattern in a reflective corneal topographer – similarly to the Placido disks shown in Fig. 2 – will not result in a sampling that ensures discrete orthogonality of the Zernike functions.

In order to benefit in reflective corneal topography from the discretization used in this paper, the optical system

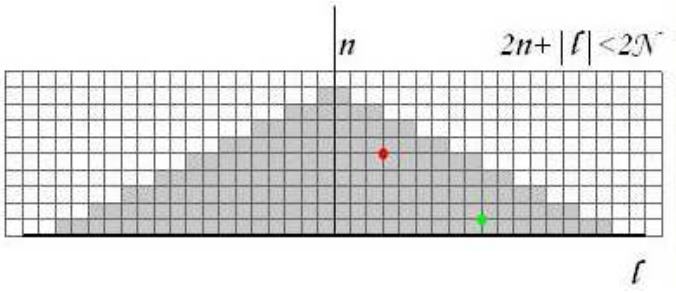

Figure 4: With the developed program, the precision of the discrete orthogonality can be checked for the mesh of points corresponding the index-set. For this index-set – i.e., for the corresponding mesh of points – and for the two Zernike functions (with the marked indices) the error was $3.8 \cdot 10^{-18}$.

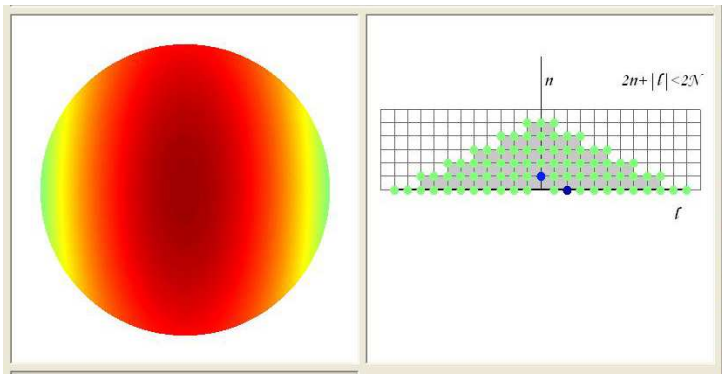

Figure 5: A sphero-cylindrical surface and its Zernike coefficients.

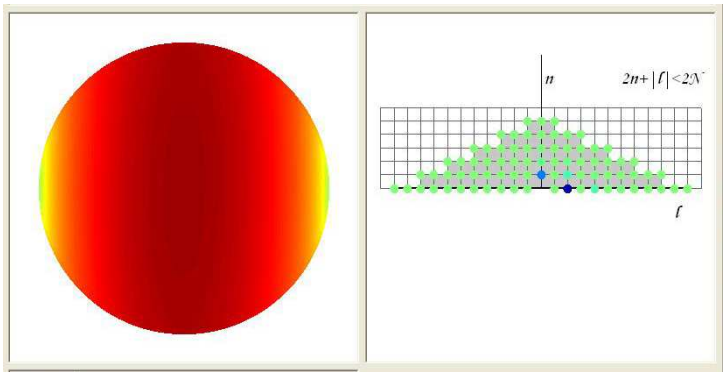

Figure 6: A more cylindrical sphero-cylindrical surface and its Zernike coefficients.

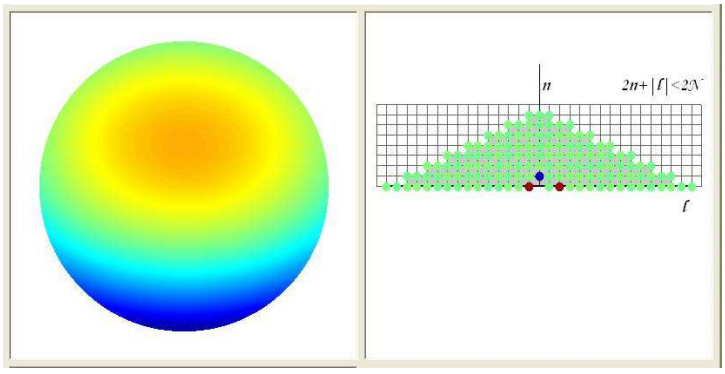

Figure 7: A surface modelling a deformed cornea (keratoconus) and its many active Zernike coefficients.

ISBN: 978-988-17012-5-1

– together with the internal control system – of the topographer must ensure that the sampling points on the corneal surface – i.e., the points (patches) that actually reflect the points of the measurement-pattern into the camera – are positioned according to the mesh with respect to the optical axis of the camera.

As the corneal surface does not have a standard shape, the above requirement is best achieved by some adaptive optical mechanism and appropriate control similarly to the approach described in [12].

References

[1] Zernike, F., "Beugungstheorie des Schneidenverfahrans und Seiner Verbesserten Form, der Phasekontrastmethode," *Physica*, V1, pp. 1137-1144, 1934.

[2] Szegö G., *Orthogonal Polynomials*. 4th Edition, AMS, New York, 1981.

[3] Wyant, J.C., Creath, K., "Basic Wavefront Aberration Theory for Optical Metrology," *Applied Optics and Optical Engineering*, V11, Academic Press, New York, 1992.

[4] Corbett, M.C., Rosen E.S., OBrart, D.P.S., *Corneal Topography: Principles and Practice*, Bmj Publ. Group, London, UK, 1999.

[5] Iskander, D.R., Collins, M.J., Davis, B., "Optimal Modeling of Corneal Surfaces with Zernike Polynomials," *IEEE Transctions on Biomedical Engineering*, V48, N11, pp. 87-95, 2001.

[6] Iskander, D.R., Morelande, M.R., Collins, M.J., Davis, B., "Modeling of Corneal Surfaces with Radial Polynomials," *IEEE Transctions on Biomedical Engineering*, V49, N11, pp. 320-328, 2002.

[7] Savarese, S. Chen, M. Perona P., "Second Order Local Analysis for 3D Reconstruction of Specular Surfaces" *IEEE 1st Int Symp 3D Data Processing Visualisation & Transmission*, 2002.

[8] Pap, M., Schipp, F., "Discrete Orthogonality of Zernike Functions," *Mathematica Pannonica*, V1, pp. 689-704, 2005.

[9] Soumelidis, A., Fazekas, Z. Schipp, F., "Surface Description for Cornea Topography Using Modified Chebyshev Polynomials, " *16th IFAC World Congress*, Prague, Czech Republic, pp. Fr-M19-TO/5, 2005.

[10] Soumelidis, A., Csákány, B., *Specification of Test Cornea Surfaces*, Project Report CORNEA-INT-2M02, MTA-SZTAKI, Budapest, Hungary, 2005.

[11] Salmon, T.O., van de Pol, C., "Normal-eye Zernike Coefficients and Root-mean-square Wavefront Errors," *Journal of Cataract & Refractive Surgery*, V32, N12, pp. 2064-2074, 2006.

[12] Ling, N., Zhang, Y., Rao, X., Wang, C., Hu, Y., Jiang. W., Jiang, C., *Adaptive Optical System for Retina Imaging Approaches Clinic Applications*, Series Springer Proceedings in Physics, Springer Verlag, Berlin, Germany, pp. 305-315, 2006.

[13] Soumelidis, A., Fazekas, Z., Schipp, F., Edelmayer, A., Németh, J., Csákány, B., "Development of a Multi-camera Corneal Topographer Using an Embedded Computing Approach," *1st Int Conf Biomedical Electronics and Devices*, Funchal, Madeira, Portugal, pp. 126-129, 2008.

[14] Fazekas, Z., Soumelidis, A., Bódis-Szomorú, A., Schipp, F., "Specular Surface Reconstruction for Multi-camera Corneal Topographer Arrangements," *30th Annual Int IEEE EMBS Conference*, Vancouver, Canada, pp. 2254-2257, 2008.